

# Downflows Under Sunspots Detected by Helioseismic Tomography

T.L. Duvall Jr.<sup>†</sup>, S. D'Silva<sup>\*</sup>, S.M. Jefferies<sup>‡</sup>, J.W. Harvey<sup>\*</sup>, & J. Schou<sup>§</sup>

<sup>†</sup> Laboratory for Astronomy and Solar Physics, NASA/Goddard Space Flight Center, Greenbelt, MD 20771 USA

<sup>‡</sup> Bartol Research Institute, University of Delaware, Newark, DE 19716 USA

<sup>\*</sup> National Solar Observatory, National Optical Astronomy Observatories, P.O. Box 26732, Tucson, AZ 85726 USA

<sup>§</sup> Stanford University, HEPL, Stanford, CA 94305-4085 USA

**How sunspots form and are maintained is one of the oldest questions in astrophysics. Using the first resolved helioseismic maps of acoustic wave travel-time we have detected evidence of strong downflows beneath sunspots and plages. These observations support Parker's model<sup>1</sup> for the formation and structure of sunspots. This model proposes that small vertical magnetic flux tubes develop downflows around them when they emerge from the deep interior of the sun where they are generated. These downflows are then able to herd a large number of small flux tubes together in a cluster to form a sunspot, which behaves as a single flux bundle as long as the inflow associated with the downflows binds them together. We estimate the flows to persist to a depth of roughly 2000 km below the solar surface with a velocity of approximately 2 km/s. The data suggest that the vertical magnetic field in the sunspot can only be a coherent flux bundle to a depth of around 600 km. Below this point however, it is possible that the downflows loosely hold a collection of small flux tubes together to form the sunspots that we see.**

The recent discovery<sup>2</sup> of how to measure the time taken by acoustic waves to travel inside the sun is a powerful tool for studying the solar interior. This new approach directly measures the travel time of acoustic waves between any point on the solar surface and a surrounding annulus. As a packet of acoustic waves propagates into the solar interior, it refracts due to the increase in sound speed until it eventually turns around and returns to the surface where it is reflected back into the interior. If the wave-packet encounters a subsurface structure, like a flow field, magnetic field, or temperature perturbation, which introduces an inhomogeneity in the wave speed along the path, its travel time will be altered. We introduce a technique to measure the alterations in the travel time at each point on the solar surface, and obtain two-dimensional maps from which we locate and measure the subsurface structures. We call this new technique helioseismic tomography, where, as in seismic tomography,<sup>3</sup> we are attempting to reconstruct the interior of the object from 1-D line integrals.

We have generated travel time maps using 1017 full-disk images, sampled once per minute in the Ca<sup>+</sup> K-line, obtained at the geographic South Pole Jan. 4-5, 1991. This series was divided into two 8.5 hour segments, to be able to test repeatability. Each segment was processed using the following procedure: (1) The images were corrected for offset and gain and the high spatial-frequency information restored to each image.<sup>4</sup> (2) The images were interpolated onto a grid of longitude  $\phi$  and  $\sin\lambda$ , where  $\lambda$  is latitude (see Fig. 1). (3) The images were filtered to isolate oscillation signals, and then spatially and temporally apodized. (4) For each time series, motions

due to a mean solar rotation were removed at each latitude separately using a Fourier shift. (5) The mean temporal crosscovariance function between each point of the images and all points of the image within a narrow annulus was computed. (6) Signal-to-noise ratio was enhanced at the expense of spatial resolution by averaging the crosscovariance functions in spatial blocks of 7 by 7 map points. (7) The crosscovariance functions were averaged, after subtraction of a mean time-distance curve in four ranges of angular distance, or annuli, (a)  $2^\circ.5-4^\circ.25$ , (b)  $4^\circ.5-7^\circ$ , (c)  $7^\circ.25-10^\circ$ , (d)  $10^\circ.25-15^\circ$ . (8) The travel times were measured from the zero crossing of the instantaneous phase of the crosscovariance function determined from a Hilbert transform technique.<sup>5</sup> (9) A ‘mean’ travel-time map was made by averaging the two sets of time measurements, corresponding to the travel time of the wave from the central point to the annulus and vice versa, and subtracting this from a map of the average of all travel times over the surface. A ‘difference’ travel-time map was made by differencing the two sets of measurements. The maps for the two 8.5 hour segments showed obvious features that rotated with the Sun and so the two were combined after a correction for solar rotation and the resultant maps are shown in Fig. 1.

The mean map indicates how subsurface structure has altered the local wave-speed from the average value. An increased wave-speed decreases the travel time, and shows up as a bright region on the mean map. The mean maps in Fig. 1 show that bright regions are correlated with the active regions in Fig. 1. The peak signal in these regions corresponds to sunspots and is roughly -0.4 min for the smallest annulus, and fades away with annulus size. This behaviour could be caused by magnetic fields which are known to alter the temperature and density of the region they occupy. Lacking a unique solution to describe the internal structure of the magnetic field we study the effect by introducing local perturbations of temperature and magnetic field separately into a solar model.<sup>6</sup> We compute the ray paths and calculate the change in travel time with and without the perturbation. The travel time decreases by about 0.4 min, if the sound speed is increased by 6% in a cylindrical region 5000 km deep and  $0^\circ.5$  in diameter about the central point. A magnetic field changes the wave speed depending on the orientation of the ray path with the field. Our calculations show that although a horizontal magnetic field can increase the effective wave speed, it cannot reproduce the observed fall off of the mean signal with increasing annulus size. A vertical magnetic field, on the other hand, can reproduce the observed trend. A signal similar to that observed can be reproduced with a field strength of 2 kG at the surface, increasing to about 4 kG at a depth of 600 km. To match the observations a weaker field would have to extend deeper (Fig. 2c). Since the typical field strength of a sunspot is 2 kG, we suggest that the mean signal is largely due to a vertical magnetic field which extends about 600 km below the solar surface.

The mean maps also show a latitudinal variation of travel time which fades with annulus size and has no obvious counterpart in the solar activity image. The almost symmetric variation about the solar equator (see Fig. 3) is reminiscent of the latitudinal variation of the wave speed perturbation derived from  $p$ -mode splittings<sup>7</sup> and of the latitudinal brightness function at this time of the solar cycle.<sup>8</sup> The mean signal in the bands is roughly -0.1 min for the smallest annulus and the bands appear to shift in latitude depending on annulus size. A 8% decrease in density scale height (which is the inverse of the density gradient with depth) caused by a vertical magnetic field would explain the magnitude of this signal. A temperature perturbation alone would not explain the band, since it would require a 2% increase in sound speed over the entire latitude band to a depth of 5000 km. Such an increase in sound speed would result in a roughly 200 K increase in surface temperature, which could have easily been detected. We speculate that these bands and the  $p$ -mode splitting perturbations share the same origin.

The difference maps detect the presence of any subsurface structure that alters the wave speed differently when the direction of the ray propagation is reversed. A flow field increases the wave speed if the ray is traveling along the flow, or decreases the wave speed if it is against the

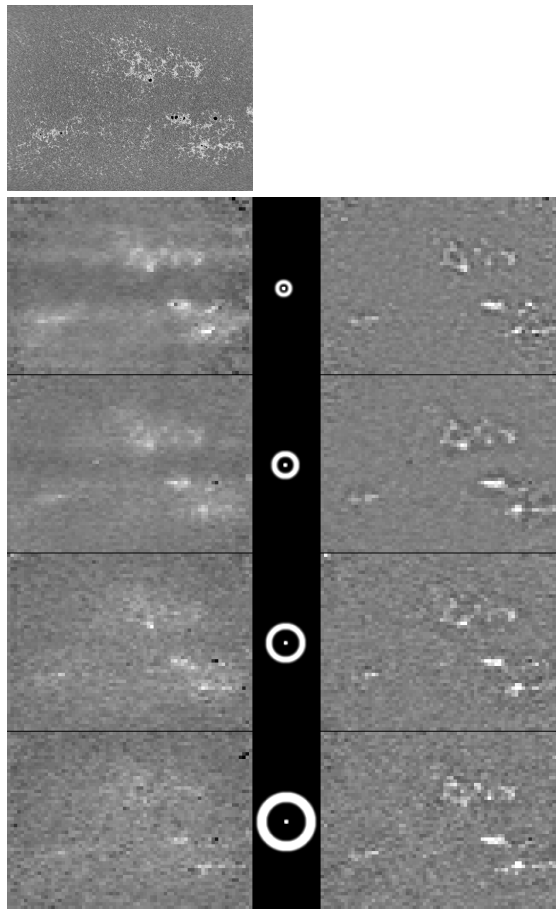


Figure 1: In the upper left is an image of the Sun at 393.3 nm ( $\text{Ca}^+$  K-line) obtained at the South Pole on Jan. 4, 1991. The image has been interpolated onto a longitude ( $\phi$ ) and sine of latitude ( $\lambda$ ) grid and only the part corresponding to the subsequent maps is shown. North is on top and west is to the right. The longitude range covered is  $\pm 62.5$  deg about the central meridian and the range in  $\sin\lambda$  is  $\pm 0.8$ . The small dark spots are sunspots which are dark because they are cooler than the surrounding surface and are the sites of the strongest magnetic fields measured on the surface. The brightenings seen in the image are called plages. They are also sites of strong magnetic fields, but not as strong as the spots, and are thought to be bright because of heating of the upper atmosphere in these regions. One of the main goals of helioseismic tomography is to understand the subsurface magnetic, thermal, and flow structure of these surface features. Below the image of the solar surface are maps of the mean and difference travel times. The left column is the mean travel time, while the right column is the difference (outward wave time - inward wave time). Longitude is along the abscissa of each map and  $\sin\lambda$  is on the ordinate with the scales being the same as for the solar image. The four maps in each column correspond to the four annuli with the smallest annulus at the top. The sizes of the annuli are shown between the two columns. The mean maps are displayed as the deviation of the travel time from the mean value for that distance. Gray is zero excess time while white features are shorter than average times. The strongest features correspond to a shorter travel time of about 0.4 min. For the difference maps, white features correspond to outward-going waves taking a shorter time than inward-going waves. The largest differences correspond to about 1 min. Noise has been estimated from the apparently random scatter in a quiet area away from the solar activity. The standard deviation is 0.03-0.04 min. for the mean maps and 0.04-0.09 min. for the difference maps with the larger values for the larger annuli.

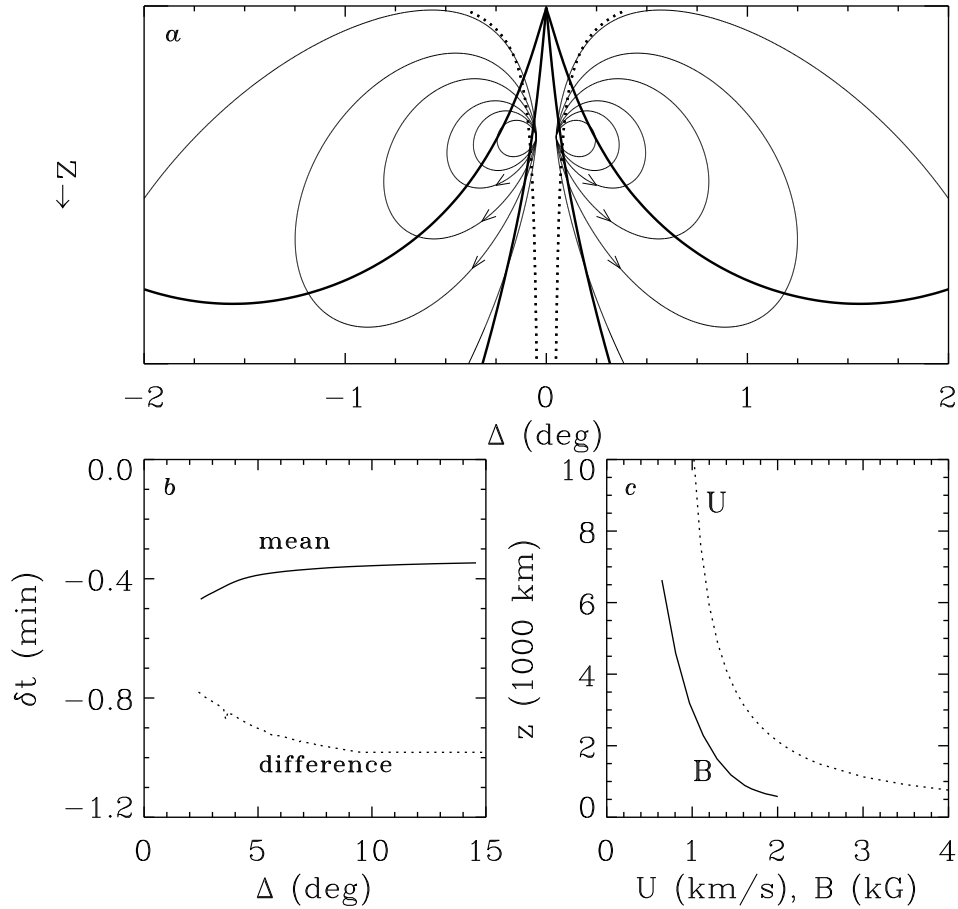


Figure 2: (a) A schematic of Parker's hypothetical downflow<sup>9</sup> around a vertical magnetic flux tube (dots) whose field strength increases with depth ( $z$ ) from the surface. ( $1 \text{ deg} \approx 12,000 \text{ km}$ ) Thick solid lines are the ray paths which reach the smallest and the largest annulus; the more vertical rays reach the largest annulus. (b) A vertical magnetic field, or a downflow is introduced in a solar model<sup>6</sup> within a cylindrical region surrounding the central point, of diameter  $0^\circ.5$ , and variable depth. The mean and difference signals are computed separately for the rays going from the central point to the annulus and back. The solid line is the mean signal as a function of annulus size for a vertical magnetic field 1000 km deep, whose surface field strength is 2 kG, and increases to 5 kG. The magnetic field region is cooled by 30% as in sunspots, and a region between 1000 km and 2500 km is heated by 15%, as heat is expected to accumulate beneath the sunspot. The dashed line is the difference signal for a 1 km/s downflow extending to a depth of 10,000 km. (c) The depth to which a vertical magnetic field should exist versus the field strength  $B$  for a family of solutions giving the same predicted signal (solid line). The depth to which a downflow should exist to give a difference signal of 1 min in the largest annulus is plotted against the downflow speed  $U$  (dashes). A 2 kG vertical magnetic field 600 km deep, and a 2 km/s downflow 2000 km deep can explain the observed mean and difference signals.

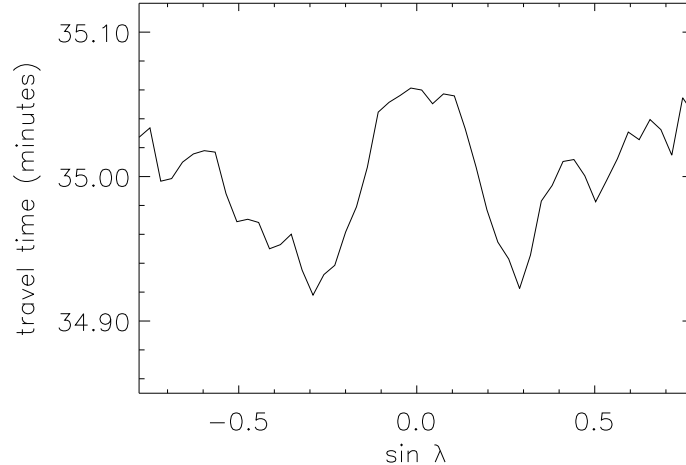


Figure 3: The travel time from the mean travel time map with smallest annulus averaged over longitude versus sine of latitude  $\lambda$ .

flow. Hence the rays traveling from the center to the annulus would have a different travel time depending on the direction of the flow. The difference signal therefore specifies the direction of the flow, measures its magnitude, and determines the size of the region to which it is confined. If the outgoing ray from a point has a shorter travel time then the difference signal is negative and shows up as a bright region on the difference map. Bright regions in the difference maps (Fig. 1) correlate with active regions in Fig. 1, indicating the presence of a flow that is directed outward from the location of the active regions. The peak difference signal is roughly -1 min in the active regions for the largest annulus, and decreases as the annulus size decreases. Horizontal outward flows are extremely unlikely as calculations demand an extraordinarily large velocity of several km/s spread over several tens of thousand km below the surface. Since the rays are largely vertical near the surface (Fig. 2a), a downflow would increase the wave speed of the outgoing ray and decrease that of the incoming ray. The dashed line in Fig. 2b shows the effect of a 1 km/s vertical downflow confined to a cylindrical region of  $0^\circ.5$  in diameter around the central point with a depth of 10,000 km. A larger flow of 2 km/s would need to persist only to about 2000 km below the surface (Fig. 2c). At the central point the rays that reach the larger annulus are more vertical and stay within the flow longer than those that reach the smaller annulus. This explains why the maximum difference signal is observed for the largest annulus. At the surface, measured horizontal flows surrounding old sunspots are opposite to the inflows expected from subsurface downflows. This suggests that the surface flows are shallow counterflow phenomena.

In summary, we have measured the acoustic wave travel time perturbations caused by subsurface structures, and have qualitatively explained the measurements in terms of downflows and magnetic fields beneath sunspots and plages, extending to a depth of about 1000 km. We are presently constrained by the low resolution of the observations from detailed mapping of the flow field and magnetic field profiles. It is tempting to believe that the sunspot which appears as a single large magnetic flux tube at the surface shreds into small flux fibers beneath this depth, and is held together as a coherent structure due to the downflows.<sup>1</sup> Moreover, downflows at a vertical

flux tube result in inflows just beneath the surface (Fig. 2a) which could herd neighbouring flux tubes and form sunspots.<sup>1</sup> This raises the question of what makes vertical magnetic flux tubes enter into either of these two distinct quasi-equilibrium states of sunspots and plages? Travel-time maps, coupled with theoretical calculations, might solve this puzzle when high resolution observations become available.

The data in the figures in this letter is available for downloading from the World-Wide Web address <http://soi.stanford.edu/~duvall/duvall.html>.

## References

1. Parker, E. N., *Astrophys. J.* **230**, 905-913 (1979).
2. Duvall, T. L. Jr., Jefferies, S. M., Harvey, J. W. & Pomerantz, M. A., *Nature* **362**, 430-432 (1993).
3. Lee, W. H. K. & Pereyra, V., *Seismic Tomography, Theory and Practice* (eds. H. M. Iyer & K. Hirahara) 9-22 (Chapman and Hall, 1993).
4. Toner, C., Jefferies, S. M. & Duvall, T. L. Jr., *Astrophys. J.* (submitted 1995).
5. Bracewell, R. N., *The Fourier Transform and Its Applications* (2nd edition, revised, McGraw-Hill, New York, 1986).
6. Bahcall, J.N. & Ulrich, R.K., *Rev. Mod. Phys.* **60**, 297-372 (1988).
7. Woodard, M. F. & Libbrecht, K. G., *Astrophys. J.* **402**, L77-L80 (1993).
8. Kuhn, J. R. & Libbrecht, K. G., *Astrophys. J.* **381**, L35-L37 (1991).
9. Parker, E. N., *Astrophys. J.* **390**, 290-296 (1992).

ACKNOWLEDGEMENTS. This work was supported in part by a grant from the National Science Foundation, by the Solar Physics Branch of the Space Physics Division of NASA, the National Solar Observatory, and by a grant from the Office of Naval Research. The National Solar Observatory is operated by the Association of Universities for Research in Astronomy, Inc., under cooperative agreement with the National Science Foundation. SD would like to thank Jacques Beckers, Bob Howard, and Jack Harvey for providing the encouragement and opportunity to pursue independent research as a post-doctoral student. TD would like to thank Phil Scherrer and the SOI group at Stanford for their hospitality during this work and for the use of their computing facilities, supported by a contract from NASA.